Check for updates

Matched Asymptotic Expansions of Unbalanced Adhesive Joints

G. Kember[1] and K. Shahin[2]

Abstract: A matched asymptotic expansion analysis is used to determine the dependence of shear stress boundary layer thickness on adhesive properties in unbalanced single-lap joints. A uniformly accurate expansion of shear stress, in a small and positive dimensionless parameter ε, is shown to contain a pair of adhesive edge boundary layers and an outer zone where the stress is slowly varying between the two layers. An overlap constraint is also found, and if it can be satisfied for $\varepsilon \ll 1$, then there is sufficient overlap and a single boundary layer of width the order of $\varepsilon^{1/2}$ at either adhesive end. The analytic results are presented in a generic format allowing their application and/or extension to similar problems. All results are numerically verified using a finite difference approximation. **DOI:** 10.1061/(ASCE)EM.1943-7889.0000574. © *2013 American Society of Civil Engineers.*

CE Database subject headings: Joints; Adhesives; Boundary layers; Shear stress.

Author keywords: Unbalanced adhesive joints; Matched asymptotic expansions; Boundary layer; Stresses.

Introduction

Adhesive bonding is increasingly used in applications involving a mix of metal and composite materials. Increased understanding of adhesive bonding has led to their use in harsh environments encountered by high-performance military aircraft and the automotive industry. Understanding adhesive joints is also important because most failures in structures originate at a joint (Gustafson et al. 2007).

Computer simulations of two-dimensional and three-dimensional configurations typically have large sets of parameters because of the complexity of adherend-adhesive mechanics and their interaction, and these parameters may be difficult to estimate. As such, the use of computer simulation models in structural design involving adhesives has been limited to special cases (Gustafson et al. 2007). More rigorous semianalytic approaches that blend asymptotic methods (Bender and Orzsag 1978; Kevorkian and Cole 1975; Barenblatt 1996) with numerical methods are in widespread use in composite and adhesive design. For example, asymptotic homogenization in composite materials whose properties have a rapid and periodic variation are constructed from numerical solutions linking local analytical solutions at the microscale to conditions applied at the macroscale (Hassan et al. 2009). Semianalytic methods are also used in adhesive bonding—for example, to derive a numerical method in an application where two elastic layers are separated by a thin adhesive layer (Klarbring and Movchan 1998).

[1]Professor, Dept. of Engineering Mathematics, Dalhousie Univ., 1340 Barrington St., Halifax, NS, Canada B3J 1B7 (corresponding author). E-mail: kembermusic@eastlink.ca

[2]Professor, Dept. of Civil Engineering, Abu-Dhabi Univ., United Arab Emirates.

Note. This manuscript was submitted on June 22, 2012; approved on November 20, 2012; published online on November 22, 2012. Discussion period open until March 1, 2014; separate discussions must be submitted for individual papers. This paper is part of the ***Journal of Engineering Mechanics***, Vol. 139, No. 10, October 1, 2013. ©ASCE, ISSN 0733-9399/2013/10-1387–1394/$25.00.

Difficulties in numerical modeling and the specific nature of their analyses has led to a continuing development and study of simplified mathematical models dedicated to modeling more generic features, and this approach complements numerical studies. As was pointed out in Shahin et al. (2008), mathematical models of adhesives may be classed into those where an entire joint and adhesive are used to find bending moments and shear forces at the ends of single-lap joints and a second group where the shear and peel stresses are examined only within the joint overlap zone. The latter group may again be subdivided into those where peel and shear stresses are decoupled and the joint is *balanced* and fully coupled models where the joint is *unbalanced*.

Purely analytical studies normally follow one of two tacks: an exact solution is found, or a special approximation is made [a full review is given in Li (2000)]. For example, an ad hoc approximation to the solution of a seventh-order unbalanced lap joint model neglecting shear deformation was first considered in Shahin et al. (2008); a full literature review is also available there). A few studies have utilized organized asymptotic methods, and these include, for example, Gilibert and Rigolot (1988), where the asymptotics of double lap joints was considered, and Banks-Sills and Salganik (1994), who modeled the asymptotics of adhesive cracks. The central difficulty with full analytic solutions is their "overwhelming complexity" (Shahin et al. 2008), which obscures how solutions functionally depend on their parameter sets, and methods specific to applications, which tend to be difficult to generalize and/or easily relate to each other, dominate the literature.

The goal of this study is to build a matched asymptotic expansion for unbalanced single-lap joints for the model presented in Shahin et al. (2008). The mathematical model includes coupled peel and shear stresses in an unbalanced joint where shear deformations are neglected. An overlap constraint is found whose satisfaction requires that the joint parameters lead to a small, positive parameter ε. Furthermore, the existence of $\varepsilon \ll 1$ guarantees (1) that a uniformly accurate approximation to shear and peel stresses in root powers of ϵ to arbitrary accuracy can be found, depending upon on our needs; (2) the existence of a single boundary layer at either endof the adhesive whose width is equal to the order of $\varepsilon^{1/2}$; and (3) that the shear deformations can be neglected.

J. Eng. Mech., 2013, 139(10): 1387-1394

Adhesive Equations

Dimensional Form

The shear stress within the adhesive layer shown in Fig. 1 is assumed to satisfy

$$\frac{d^7\tau}{dx^7} - \alpha_1\frac{d^5\tau}{dx^5} + \eta_1\frac{d^3\tau}{dx^3} - (\eta_1\alpha_1 + \eta_2\alpha_2)\frac{d\tau}{dx} = 0 \tag{1}$$

subject to the seven conditions

$$\int_{-c}^{c} \tau(x)\, dx = -P \tag{2}$$

$$\left.\frac{d\tau}{dx}\right|_{\mp c} = A_{1,2} \tag{3}$$

$$\left.\frac{d^5\tau(x)}{dx^5}\right|_{\mp c} - \alpha_1\left.\frac{d^3\tau(x)}{dx^3}\right|_{\mp c} = \mp B_{1,2} \tag{4}$$

$$\left.\frac{d^6\tau(x)}{dx^6}\right|_{\mp c} - \alpha_1\left.\frac{d^4\tau(x)}{dx^4}\right|_{\mp c} - \alpha_2\eta_2\tau(x)|_{\mp c} = \mp B_{3,4} \tag{5}$$

where $\mp B_{1,2}$ means $-B_1$ at $x = -1$, $+B_2$ at $x = +1$ and similarly for $\mp B_{3,4}$, and the sign of α_2 used here is minus the same parameter as in Shahin et al. (2008). The first condition is a so-called load condition. and the remaining six conditions are split between, and applied at, the endpoints $x = \pm 1$.

To be clear, the main features of this model are discussed; note that full details of the analytical model are given in Shahin et al. (2008). Stresses within the adhesive layer are considered here for a single-lap joint model, depicted in Fig. 1. The lap joint deformations are assumed to be small enough to allow a reduction to the consideration of axially varying adhesive stress within the adhesive layer. This assumption is verified in Shahin et al. (2008), where the effects of geometric nonlinearity are investigated using a finite element model of the lap joint that includes the adherends and adhesive layer. The joint parameters $\alpha_1, \alpha_2, \eta_1$, and η_2 in Eq. (1) depend upon the physical properties of the upper and lower adherends and adhesive layers (see Fig. 1 and Table 1) and the extensional, coupling, and flexural stiffnesses of the adherends computed, as in Shahin et al. 2008), from the adherend physical properties.

In the analytical model, the adhesive stresses are found only within the adhesive layer—that is, the analytical model extends only over the range $-c \le x \le c$ in Fig. 1. Seven boundary conditions are therefore specified for the range $-c \le x \le c$, with six applied at the ends of the adhesive and one distributed over the adhesive. The first boundary condition ensures equilibrium of forces in the shear stress plane. The second and third conditions relate the shear stress gradient at the two boundaries to the two constants $A_{1,2}$ that represent the difference in the axial strains between the adherends. In the fourth and fifth boundary conditions, the terms $B_{1,2}$ represent the influence of curvature of the adherends on the adhesive peel stress gradient. Finally, the sixth and seventh conditions represent the effects of the end shear forces on the adhesive peel stress represented in the constants $B_{3,4}$.

The accuracy of the analytical model hinges on the ability to specify the edge forces and bending moments at the adhesive ends as represented in the constants $A_{1,2}$, $B_{1,2}$, and $B_{3,4}$, and their computation is in Shahin et al. (2008). Furthermore, a large literature devoted to this topic on single-lap joints and developments for other configurations can be found in Li (2000).

Dimensionless Form

The adhesive length is scaled with respect to the half-length c using the dimensionless length variable $X = x/c$, while the shear stress $\tau(x)$ is rescaled in terms of the force per unit length P applied to the adhesive as $Y = \tau/(P/c)$, yielding

$$\frac{d^7Y(X)}{dX^7} - \alpha_1 c^2\frac{d^5Y(X)}{dX^5} + \eta_1 c^4\frac{d^3Y(X)}{dX^3} - (\eta_1\alpha_1 + \eta_2\alpha_2)c^6\frac{dY(X)}{dX} = 0 \tag{6}$$

subject to the seven conditions

$$\int_{-1}^{1} Y(X)\, dX = -1 \tag{7}$$

$$\left.\frac{dY}{dX}\right|_{\mp 1} = \frac{c^2 A_{1,2}}{P} \tag{8}$$

$$\left.\frac{d^5Y(X)}{dX^5}\right|_{\mp 1} - \alpha_1 c^2\left.\frac{d^3Y(X)}{dX^3}\right|_{\mp 1} = \frac{\mp c^6 B_{1,2}}{P} \tag{9}$$

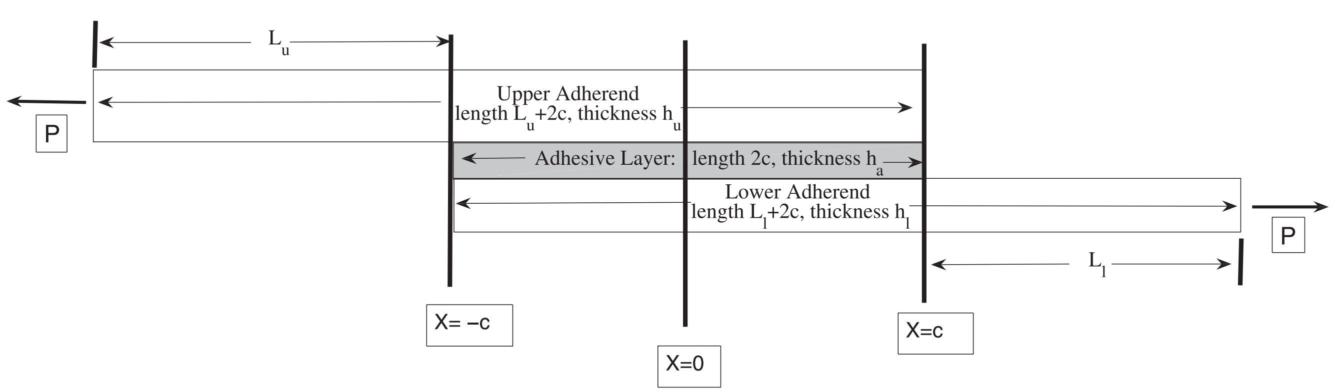

Fig. 1. The adhesive layer, upper adherend, and lower adherend are depicted for a single-lap joint

J. Eng. Mech., 2013, 139(10): 1387-1394

Table 1. Physical Parameters and Computed Dimensional Parameter Values, after Shahin et al. (2008) for Fig. 2

Physical parameter	Value
E_u	70,000 MPa
E_l	130,000 MPa
G_a	385 MPa
h_u	5 mm
h_l	5 mm
h_a	0.3 mm
L_u	100 mm
L_l	100 mm
c	50 mm
P	500 N/mm
Computed parameter	**Value**
α_1	$2.14 \cdot 10^{-2}$ 1/mm^2
α_2	$1.85 \cdot 10^{-3}$ 1/mm^3
η_1	$6.4 \cdot 10^{-3}$ 1/mm^4
η_2	$5.09 \cdot 10^{-3}$ 1/mm^3
A_1	4.09 N/mm^3
A_2	-2.36 N/mm^3
B_1	$4.66 \cdot 10^{-3}$ N/mm^7
B_2	$-2.81 \cdot 10^{-2}$ N/mm^7
B_3	$1.18 \cdot 10^{-5}$ N/mm^8
B_4	$5.43 \cdot 10^{-5}$ N/mm^8

Note: E_u and E_l are the elastic moduli of the upper and lower adherends, respectively, and G_a is the adhesive shear modulus. The computed parameters are referred to within the text.

$$\left.\frac{d^6Y(X)}{dX^6}\right|_{\mp 1} - \alpha_1 c^2 \left.\frac{d^4Y(X)}{dX^4}\right|_{\mp 1} - \alpha_2\eta_2 c^6 Y(X)\big|_{\mp 1} = \frac{\mp c^7 B_{3,4}}{P} \quad (10)$$

Matched Asymptotic Expansion

The matched asymptotic expansion proceeds by first constructing an *outer solution*, valid away from the endpoints, that depends on the outer variable X. This is followed by two *boundary layer* or *inner solutions* valid near each endpoint. Because six conditions are applied at the endpoints and the integral load condition requires a solution that is valid over the entire domain, none of the seven conditions can be applied to the outer solution. Hence, the outer solution is constructed from an asymptotic expansion of the differential equation and satisfies no conditions. The endpoint conditions are all referred to their respective boundary layer solutions, and the load condition is finally satisfied after the construction of a uniformly valid composite solution from the formal union (Van Dyke 1975) of the set of outer and boundary layer solutions.

To begin, note that substituting the dimensional parameters in Table 1 to the model in Eq. (6) indicates that the magnitude of the coefficients of the third, fifth, and seventh derivatives scale, respectively, as $O(10^2)$, $O(10^4)$, and $O(10^6)$, where O means "the order of". This suggests that these three quantities can be defined in the form

$$\alpha_1 c^2 = \frac{M_1}{\varepsilon}$$
$$\eta_1 c^4 = \frac{M_2}{\varepsilon^2} \quad (11)$$
$$(\eta_1\alpha_1 + \eta_2\alpha_2)c^6 = \frac{M_3}{\varepsilon^3}$$

where choosing $\varepsilon = 0.01$ yields the order-one constants $M_1 = 0.536$, $M_2 = 4.00$, and $M_3 = 2.29$. It is shown here that the power law relationship defined in Eq. (11), for the parameter choices in Table 1, leads to a boundary layer of width $O(\varepsilon^{1/2}) = O(0.1)$, wherein the shear and peel stresses are strongly coupled with a balanced sensitivity to all parameters in Eq. (6). Eq. (11) will be referred to as the *overlap constraint*.

Substituting to Eq. (6) and dividing by the largest parameter

$$\frac{dY(X)}{dX} - \frac{\varepsilon M_2}{M_3}\frac{d^3Y(X)}{dX^3} + \frac{\varepsilon^2 M_1}{M_3}\frac{d^5Y(X)}{dX^5} - \frac{\varepsilon^3}{M_3}\frac{d^7Y(X)}{dX^7} = 0 \quad (12)$$

Outer Solution

The outer solution is a regular perturbation expansion, and the form of Eq. (12) suggests that the expansion is in integer powers of ε. However, further analysis will show that in fact the series proceeds in root powers, and although this could be discovered later upon satisfaction of the dimensionless load condition, it is convenient to use this form now

$$Y(X) = Y_0(X) + \varepsilon^{1/2}Y_1(X) + \varepsilon Y_2(X) + \cdots \quad (13)$$

Substitution of the first two terms of Eq. (13) to Eq. (12) with the assumption that all of the derivative terms are order one yields the $O(\varepsilon)$ expansion

$$Y(X) = G_0 + \varepsilon^{1/2}G_1 + O(\varepsilon) \quad (14)$$

where G_0 and G_1 are constants to satisfy $dY_0(X)/dX = dY_1(X)/dX = 0$.

The dominance of the constant approximation to the outer solution $Y(X)$ has occurred because the higher derivatives are increasingly smaller away from the boundaries $X = \pm 1$. A consequence is that the constant approximation cannot satisfy the conditions near $X = \pm 1$ and is invalid there. Within the immediate vicinity of $X = \pm 1$, the solution is rapidly varying away from the constant approximation to satisfy the conditions. The solution near the boundaries, $X = \pm 1$, is split into two boundary layer or inner solutions valid near each instance of $X = \pm 1$.

Inner Solutions

Near each of the boundaries $X = \pm 1$, respectively, is defined an order-one, or *stretched* variable $(1 \mp X)/a(\varepsilon)$ that is order one within $O[a(\varepsilon)] \ll 1$ of $X = \pm 1$.

Inner Differential Equations

The *right* inner solution $V_R(Z_R)$ valid near $X = 1$ has the inner variable $Z_R = (1 - X)/a(\varepsilon)$, and the subscript R refers to *right*. Note that the outer dependent variable Y in Eq. (6) has been renamed V_R for clarity in delineating the outer and inner solutions.

Rewriting Eq. (12) in terms of Z_R, and multiplying by M_3/ε^3,

$$\frac{d^7V_R(Z_R)}{dZ_R^7} - M_1\frac{a^2(\varepsilon)}{\varepsilon}\frac{d^5V_R(Z_R)}{dZ_R^5} + M_2\frac{a^4(\varepsilon)}{\varepsilon^2}\frac{d^3V_R(Z_R)}{dZ_R^3} - M_3\frac{a^6(\varepsilon)}{\varepsilon^3}\frac{dV_R(Z_R)}{dZ_R} = 0 \quad (15)$$

For order-one M_1, M_2, and M_3, it is possible to choose $a(\varepsilon)$ in such a way that *all terms* in Eq. (15) are of equal order—that is, balanced, and this occurs when $a(\varepsilon) = (\varepsilon^{1/2}) = 0.1$

J. Eng. Mech., 2013, 139(10): 1387-1394

$$\frac{d^7V_R(Z_R)}{dZ_R^7} - M_1\frac{d^5V_R(Z_R)}{dZ_R^5} + M_2\frac{d^3V_R(Z_R)}{dZ_R^3} - M_3\frac{dV_R(Z_R)}{dZ_R} = 0 \quad (16)$$

The order-one uniformity in the magnitude of M_1, M_2, and M_3 is a *generic* feature of the strong coupling between the peel and shear stresses within $O(\varepsilon^{1/2}) = O(0.1)$ of the boundaries $X = \pm 1$. Note also that if order-one M_i, $i = 1,2,3$ are not available, then the full balancing in Eqs. (15) and (16) cannot occur, and nested boundary layers (Kevorkian and Cole 1975) may result, with undesirable variation in stress gradients.

Proceeding similarly near $X = -1$, the *left* inner variable is $Z_L = (1+X)/(\varepsilon^{1/2})$, and the *left* inner solution $V_L(Z_L)$ satisfies

$$\frac{d^7V_L(Z_L)}{dZ_L^7} - M_1\frac{d^5V_L(Z_L)}{dZ_L^5} + M_2\frac{d^3V_L(Z_L)}{dZ_L^3} - M_3\frac{dV_L(Z_L)}{dZ_L} = 0 \quad (17)$$

Inner Conditions

There are seven conditions that must be satisfied by the asymptotic expansion. The six boundary conditions are split between $V_R(Z_R)$ at $X = 1$ and $V_L(Z_L)$ at $X = -1$. The seventh condition is a distributed load condition to be satisfied by a composite solution that is uniformly valid over the entire range of X. The composite solution will be built from a union of the outer and inner solutions after they are found.

The three conditions in Eqs. (8) to (10) applied at $X = 1$ are written in terms of the inner independent variable $Z_R = (1-X)/a(\varepsilon)$, and recall that the outer variable Y in Eq. (6) is renamed V_R for clarity,

$$\begin{aligned}
&\left.\frac{dV_R(Z_R)}{dZ_R}\right|_{Z_R=0} = -\frac{a(\varepsilon)c^2A_2}{P}\\
&\left.\frac{d^5V_R(Z_R)}{dZ_R^5}\right|_{Z_R=0} - a^2(\varepsilon)\alpha_1c^2\left.\frac{d^3V_R(Z_R)}{dZ_R^3}\right|_{Z_R=0} = -\frac{a^5(\varepsilon)c^6B_2}{P}\\
&\left.\frac{d^6V_R(Z_R)}{dZ_R^6}\right|_{Z_R=0} - a^2(\varepsilon)\alpha_1c^2\left.\frac{d^4V_R(Z_R)}{dX^4}\right|_{Z_R=0}\\
&\qquad - a^6(\varepsilon)\alpha_2c^6\eta_2V_R(Z_R)|_{Z_R=0} = \frac{a^6(\varepsilon)c^7B_4}{P}
\end{aligned} \quad (18)$$

The order-one parameters associated with the right-hand side of Eq. (18) are defined as

$$\tilde{A}_2 = \frac{a(\varepsilon)c^2A_2}{P}, \quad \tilde{B}_2 = \frac{a^5(\varepsilon)c^6B_2}{P}, \quad \tilde{B}_4 = \frac{a^6(\varepsilon)c^7B_4}{P} \quad (19)$$

and then

$$\begin{aligned}
&\left.\frac{dV_R(Z_R)}{dZ_R}\right|_{Z_R=0} = -\tilde{A}_2\\
&\left.\frac{d^5V_R(Z_R)}{dZ_R^5}\right|_{Z_R=0} - M_1\left.\frac{d^3V_R(Z_R)}{dZ_R^3}\right|_{Z_R=0} = -\tilde{B}_2\\
&\left.\frac{d^6V_R(Z_R)}{dZ_R^6}\right|_{Z_R=0} - M_1\left.\frac{d^4V_R(Z_R)}{dZ_R^4}\right|_{Z_R=0} - M_4V_R(Z_R)|_{Z_R=0} = \tilde{B}_4
\end{aligned} \quad (20)$$

where the left-hand side has $M_4 = a^6(\varepsilon)c^6\alpha_2\eta_2$. Substituting from Table 1 and noting that $a(\varepsilon) = \varepsilon^{1/2} = 0.1$, we have $\tilde{A}_2 = -1.118$, $\tilde{B}_2 = -0.879$, $\tilde{B}_4 = 0.0848$, and $M_4 = 0.147$.

The three conditions applied at $X = -1$ and satisfied by $V_L(Z_L = 0)$ are treated similarly and so the order-one parameters are defined as

$$\tilde{A}_1 = \frac{a(\varepsilon)c^2A_1}{P}, \quad \tilde{B}_1 = \frac{a^5(\varepsilon)c^6B_1}{P}, \quad \tilde{B}_3 = \frac{a^6(\varepsilon)c^7B_3}{P} \quad (21)$$

which gives the conditions applied to $V_L(Z_L = 0)$ as

$$\begin{aligned}
&\left.\frac{dV_L(Z_L)}{dZ_L}\right|_{Z_L=0} = -\tilde{A}_1\\
&\left.\frac{d^5V_L(Z_L)}{dZ_L^5}\right|_{Z_L=0} - M_1\left.\frac{d^3V_L(Z_L)}{dZ_L^3}\right|_{Z_L=0} = -\tilde{B}_1\\
&\left.\frac{d^6V_L(Z_L)}{dZ_L^6}\right|_{Z_L=0} - M_1\left.\frac{d^4V_L(Z_L)}{dZ_L^4}\right|_{Z_L=0} - M_4V_L(Z_L)|_{Z_L=0} = \tilde{B}_3
\end{aligned} \quad (22)$$

Again, substituting from Table 1 and noting that $a(\varepsilon) = \varepsilon^{1/2} = 0.1$ we have $\tilde{A}_1 = 2.05$, $\tilde{B}_1 = 1.46$, and $\tilde{B}_3 = 0.184$, and $M_4 = 0.147$ is unchanged from before.

Determining Inner Solutions

The inner expansions of $V_R(Z_R)$ and $V_L(Z_L)$ take the same form as the outer expansion in Eq. (13)

$$V_R(Z_R) = V_{0R}(Z_R) + \varepsilon^{1/2}V_{1R}(Z_R) + O(\epsilon) \quad (23)$$

and similarly for $V_L(Z_L)$.

The differential equation satisfied by the inner solutions is homogeneous, and because the same form is satisfied by all components $V_i(Z_R)$, $i = 1,2,3,\ldots$, we have $V_i(Z_R) = \exp(\lambda Z_R)$. Substituting to Eq. (16) and setting $\Lambda = \lambda^2$ and removing the root $\lambda = 0$, the inner solution characteristic equation is

$$\Lambda^3 - M_1\Lambda^2 + M_2\Lambda - M_3 = 0 \quad (24)$$

This third-order polynomial has a known closed solution, and for the parameters M_i, $i = 1,2,3$ considered here, we find that $\Lambda_1 = 0.5698$, while the remaining roots are $\Lambda_{2,3} = -0.0170 \pm 2.005\mathbf{i}$. Referring to $\lambda = \Lambda^{1/2}$, and keeping roots with minus real part, we find that $\lambda_1 = -0.7549$ and $\lambda_{2,3} = -1.00 \pm 1.01\mathbf{i}$, recalling that $\lambda_0 = 0$. The three remaining roots with positive real part are exponentially large for large Z_R and Z_L and must be discarded, as shown later, leaving the inner solution dependent upon four roots.

J. Eng. Mech., 2013, 139(10): 1387-1394

The inner solutions $V_{0R}(Z_R)$ and $V_{0L}(Z_L)$ each have four free constants that are, respectively, determined by substitution to Eqs. (20) and (22). These solutions are greatly simplified by noting that the complex conjugate eigenvalues and the appearance of only odd or even derivatives within each condition lead to

$$\begin{aligned} V_R(Z_R) &\approx V_{0R}(Z_R) + \sqrt{\varepsilon} V_{1R}(Z_R) \\ &= C_{0R} + C_{1R} e^{\lambda_1 Z_R} + C_{2R} e^{\lambda_2 Z_R} + C_{2R}^* e^{\lambda_2^* Z_R} \\ &+ \sqrt{\epsilon}\left(D_{0R} + D_{1R} e^{\lambda_1 Z_R} + D_{2R} e^{\lambda_2 Z_R} + D_{2R}^* e^{\lambda_2^* Z_R}\right) \end{aligned} \tag{25}$$

where the superscript starred notation denotes the complex conjugate. A similar form is satisfied by $V_L(Z_L)$.

Matching

The outer solution $Y(X)$ is functionally matched with the inner solutions $V_R(Z_R)$ and $V_L(Z_L)$ in a region of overlapping validity following the approach in Van Dyke (1975). Briefly, the procedure has two steps: (1) outer and inner solutions are written in complementary variables and the limit $\varepsilon \to 0$ is taken; and (2) either the outer or inner solution is returned to its original variable and the limiting results are equated.

To be clear, the sequential nature of the matching is shown by first matching $Y(X) \approx G_0$ with $V_R(Z_R)$ in (25). Writing $Y(X)$ in terms of the inner variable Z_R yields $Y(Z_R) \approx G_0$, and proceeding similarly for the inner solution,

$$\begin{aligned} V_R(X) \approx V_{0R}(Z_R) &= C_{0R} + C_{1R} e^{\lambda_1 (1-X)/\sqrt{\varepsilon}} + C_{2R} e^{\lambda_2 (1-X)/\sqrt{\varepsilon}} \\ &+ C_{2R}^* e^{\lambda_2^* (1-X)/\sqrt{\varepsilon}} \end{aligned} \tag{26}$$

In the limit $\varepsilon \to 0$, $V_R(X) \approx C_{0R}$, and the exponentially small terms have been dropped. At this stage, it is clear that if the eigenvalues with positive real part had been retained earlier, then they would have been exponentially large outside the boundary layer, and in the matching process, they would have been removed by zeroing their coefficients.

Returning either $Y(Z_R)$ or $V_R(X)$ to their original variables and equating gives $C_{0R} = G_0$; note that we are choosing, for clarity, to work with the outer solution constants. Next, an analogous match of the inner solution $V_L(Z_L)$ with $Y(X)$ leads to $C_{0L} = G_0$, and thus the asymptotic solution to $O(\varepsilon^{1/2})$ is

$$V_L(Z_L) \approx V_{0L}(Z_L) = G_0 + C_{1L} e^{\lambda_1 Z_L} + C_{2L} e^{\lambda_2 Z_L} + C_{2L}^* e^{\lambda_2^* Z_L} \tag{27}$$

$$Y(X) \approx Y_0(X) = G_0 \tag{28}$$

$$V_R(Z_R) \approx V_{0R}(Z_R) = G_0 + C_{1R} e^{\lambda_1 Z_R} + C_{2R} e^{\lambda_2 Z_R} + C_{2R}^* e^{\lambda_2^* Z_R} \tag{29}$$

The constant G_0 will be determined from the distributed load condition [Eq. (7)] after a composite solution is constructed.

Composite Solution and Load Condition

The dimensionless load condition in Eq. (7) remains to be satisfied. A uniformly valid composite solution $Y^{(c)}(X)$ —that is, valid over $-1 \leq X \leq 1$ to uniform accuracy, is used to satisfy the distributed load condition in Eq. (7) and thus determine the free constant G_0.

$Y^{(c)}(X)$ is formally defined as the union (Van Dyke 1975) of $V_L(Z_L)$, $Y(X)$, and $V_R(Z_R)$. The outer and inner solutions are assumed to *intersect* in the two boundary layer regions of overlapping validity where they were functionally matched. In this case, the intersection is just G_0 in each boundary layer, for a total of $2G_0$, giving $Y^{(c)}(X) = Y_0(X) + V_{0L}(Z_L) + V_{0R}(Z_R) - 2G_0$ and

$$\begin{aligned} Y^{(c)}(X) \approx G_0 &+ C_{1L} e^{\lambda_1 Z_L} + C_{2L} e^{\lambda_2 Z_L} + C_{2L}^* e^{\lambda_2^* Z_L} + C_{1R} e^{\lambda_1 Z_R} \\ &+ C_{2R} e^{\lambda_2 Z_R} + C_{2R}^* e^{\lambda_2^* Z_R} + O\left(\sqrt{\varepsilon}\right) \end{aligned} \tag{30}$$

where $Z_L = (1+X)/(\varepsilon^{1/2})$ and $Z_R = (1-X)/(\varepsilon^{1/2})$.

Note that the six constants, each determined from the solution of a linear system of three equations, that multiply the exponentially small terms are dependent on G_0 —that is, G_0 sits in the third condition [Eqs. (20) and (22)] as part of $V_R(Z_R = 0)$ and $V_L(Z_L = 0)$. Each set of three constants in $V_R(Z_R)$ and $V_L(Z_L)$ may be, respectively, determined from Eqs. (20) and (22) *after* the discovery of G_0.

To find G_0, the composite solution in Eq. (30) is substituted to Eq. (7), and after integrating, simplifying, and working to algebraic accuracy,

$$2G_0 = -1 + 2\sqrt{\varepsilon}\,\Re\left(\frac{C_{1L} + C_{1R}}{\lambda_1} + \frac{C_{2L} + C_{2R}}{\lambda_2} + \frac{C_{3L} + C_{3R}}{\lambda_3}\right) \tag{31}$$

Equating order-one coefficients clearly gives $G_0 = -1/2$.

Now that $G_0 = -1/2$ is known, we can independently solve for the three constants in each of the inner solutions $V_L(Z_L)$ and $V_R(Z_R)$ by substituting from Eqs. (29) to (20) and Eqs. (27) to (22).

Going to Higher Order

This approach to the construction and matching of the outer and inner solutions has followed a sequence where G_0 of the outer solution is found from the load condition, after which the two sets of three constants in the inner approximations $V_{0L}(Z_L)$ and $V_{0R}(Z_R)$ are independently determined.

This procedure is continued to next order—that is, $O(\varepsilon^{1/2})$, and note that the result will be $O(\varepsilon)$ because that is the size of the correction term. Recall that $V_{1R}(Z_R)$ and $V_{1L}(Z_L)$ of the inner expansion in Eq. (23) satisfy the *same* differential Eq. (17) and therefore have the same form as $V_{0R}(Z_R)$ and $V_{0L}(Z_L)$.

Proceeding as before, we find that G_1 is the one-half the coefficient of $\varepsilon^{1/2}$ on the right-hand side of Eq. (31). Furthermore, the two sets of three unknown constants D_{iR}, D_{iL} in $V_{1R}(Z_R)$, and $V_{1L}(Z_L)$ satisfy their respective conditions in Eqs. (20) and (22). Substitution of the inner expansion [Eq. (23)] to the conditions and equating coefficients of $\varepsilon^{1/2}$ yields the conditions applied to $V_{1R}(Z=0)$

$$\begin{aligned} &\left.\frac{dV_{1R}(Z_R)}{dZ_R}\right|_{Z_R=0} = 0 \\ &\left.\frac{d^5 V_{1R}(Z_R)}{dZ_R^5}\right|_{Z_R=0} - M_1 \left.\frac{d^3 V_{1R}(Z_R)}{dZ_R^3}\right|_{Z_R=0} = 0 \\ &\left.\frac{d^6 V_{1R}(Z_R)}{dZ_R^6}\right|_{Z_R=0} - M_1 \left.\frac{d^4 V_{1R}(Z_R)}{dZ_R^4}\right|_{Z_R=0} = M_4 G_1 \end{aligned} \tag{32}$$

while an identical form is applied to $V_{1L}(Z_L = 0)$ with R replaced by L. The symmetry of the boundary conditions beyond the zeroth term means that higher order corrections to the inner solution are entirely symmetric and the constants D_{iR} are equal to D_{iL}.

J. Eng. Mech., 2013, 139(10): 1387-1394

Discussion

The composite asymptotic expansion found here is presented in Figs. 2 and 3 for parameters, respectively, from Tables 1 and 2. In both figures, a comparison is made between a standard finite difference solution of the dimensionless shear stress equations for two cases: (1) the one-term $O(\varepsilon^{1/2})$ approximation; and (2) the two-term $O(\varepsilon)$ approximation. The lower accuracy $O(\varepsilon^{1/2})$ seen in the one-term approximations is as expected from the expansion, and the two-term expansions are of uniformly higher accuracy.

The shear stress boundary layer width is qualitatively equal to $O(\varepsilon^{1/2}) = O[(0.01)^{1/2}] = O(0.1)$ in Fig. 2 and $O(\varepsilon^{1/2}) = O[(0.001)^{1/2}] = O(0.03)$ in Fig. 3 as predicted from the asymptotics. Note also that in Fig. 3, the two-term matched asymptotic expansion is able to represent the rapid variation of the dimensionless shear stess just inside the $x = -1$ end and to capture both its peak and location.

Satisfaction of the overlap constraint [Eq. (11)] for $\varepsilon \ll 1$ is consistent with order-one M_1, M_2 and M_3 and a full balancing of all terms within the boundary layer. For the two parameter sets, $\varepsilon \ll 1$ does exist, and therefore there is sufficient overlap within the joint for a single boundary layer to exist at either end. If $\varepsilon \ll 1$ does not exist, then the full balancing in Eqs. (15) and (16) cannot occur, and a single boundary layer would possibly give way to multiple, nested boundary layers (Kevorkian and Cole 1975) depending upon the choice of parameters. Stated another way, nested boundary layers may occur for parameter sets that lead to different orders of magnitude for M_1, M_2 and M_3 in the overlap constraint [Eq. (11)]. Such nested layers are likely to show undesirable variations in stress gradients in the adhesive joint. Satisfaction of this constraint and the resulting full balancing justifies neglecting shear deformations—that is, finite element numerical approximations including shear deformations were found in Shahin et al. (2008) to provide qualitative agreement with the mathematical model neglecting shear when full balancing occurred. The overlap constraint is also useful for design because it predicts parameter sets that lead to the existence of boundary layers that are not nested at either adhesive edge along with the width of the boundary layers, all without access to the solutions.

Conclusions

A matched asymptotic expansion analysis was used to express the dependence of the dimensionless shear stress boundary layer thickness on adhesive properties in unbalanced single-lap joints. Comparison with numerical solutions demonstrated that the two-term asymptotic expansions give uniformly and highly accurate results while the boundary layer width qualitatively is $O(\varepsilon^{1/2})$, as predicted. Adhesive edge boundary layers bounding an outer zone wherein the stresses are slowly varying were shown to exist if a small parameter $\varepsilon \ll 1$ could be found that satisfies an overlap constraint consisting of three equations. Satisfaction of the overlap constraint implies there is sufficient joint overlap and justifies neglecting shear deformations. The analytic results were presented in a generic format to allow the application of this method to similar

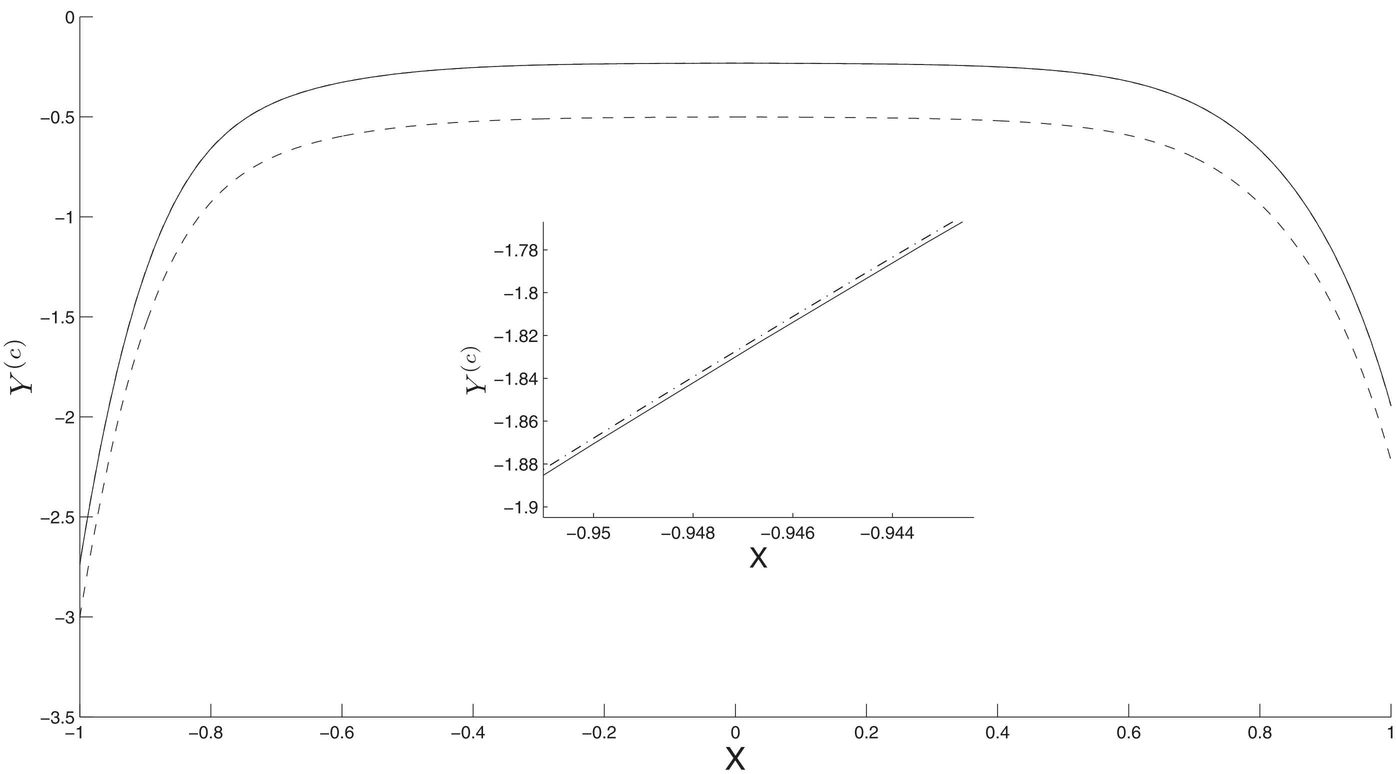

Fig. 2. A standard finite difference numerical approximation to the dimensionless shear stress is shown as a solid line; the one-term asymptotic expansion $Y^{(c)}$ from Eq. (30) is shown as a dashed line and is uniformly accurate to $O(\varepsilon^{1/2}) = O(0.1)$, as predicted.; the two-term $O(\varepsilon) = O(0.01)$ approximation, developed in the text and that includes the $O(\varepsilon^{1/2})$ term in Eq. (30) (dashed-dotted line), is nearly superimposed by the numerical solution (solid line); the boundary layer width $O(\varepsilon^{1/2}) = O(0.1)$, predicted by the asymptotic solution, is the region of steep shear stress gradient; the existence of a single boundary layer is guaranteed by the existence of order-one constants $M_1 = 0.536$, $M_2 = 4.00$, and $M_3 = 2.29$ that satisfy the overlap constraint [Eq. (11)]

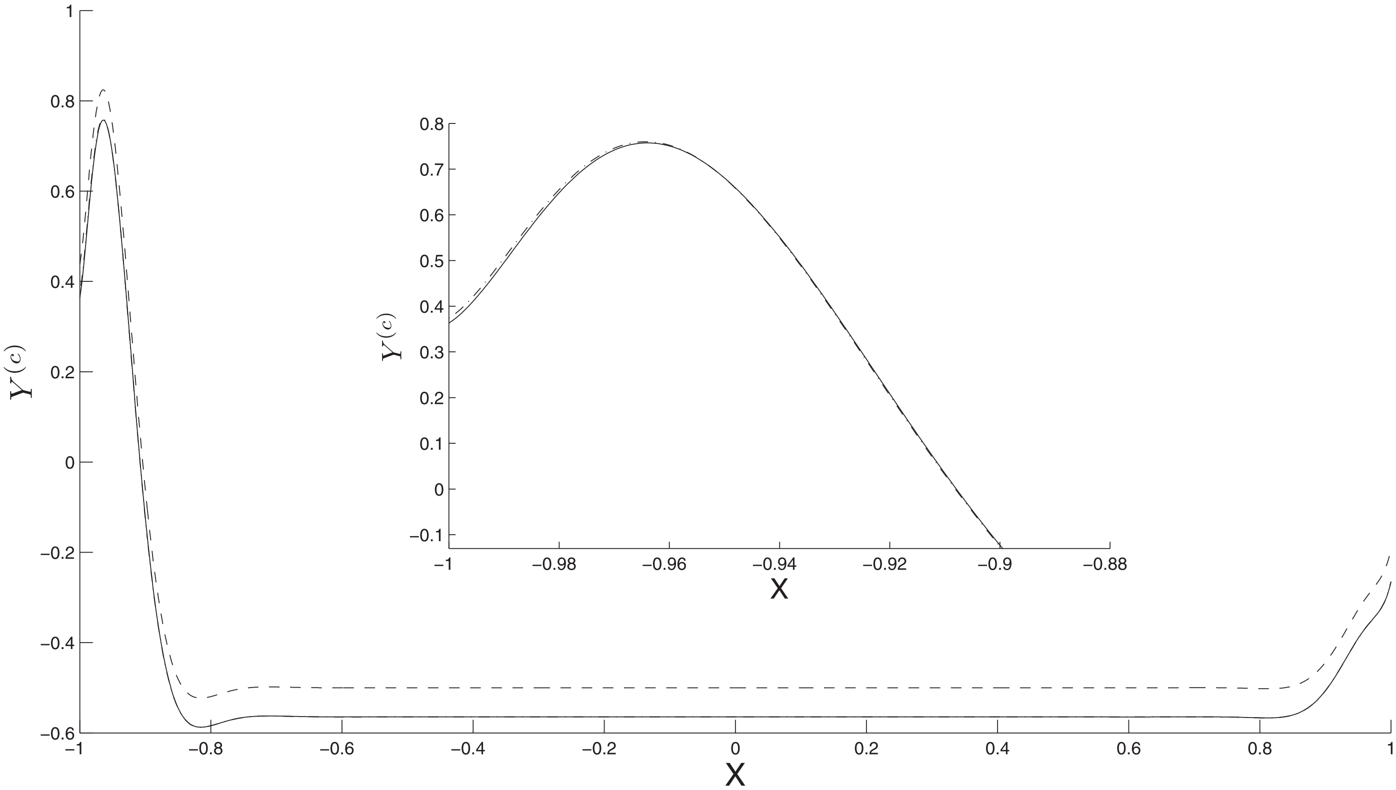

Fig. 3. Figure is organized in the same way as Fig. 2, with parameters given in Table 2; the dimensionless shear stress $Y^{(c)}$ boundary layer width $O(\varepsilon^{1/2}) = O[(0.001)^{1/2}] = O(0.03)$, predicted by the asymptotic solution, is the region of steepest shear stress gradient; the existence of a single boundary layer at either end is guaranteed by the existence of order-one constants $M_1 = 0.934$, $M_2 = 1.73$, and $M_3 = 2.29$ that satisfy the overlap constraint [Eq. (11)] for $\epsilon = 0.001$; note that the asymptotic expansion captures the sharp peak near $x = -1$ in the shear stress, that is, the numerical solution and two-term asymptotic expansion are nearly superimposed in the inset figure

Table 2. Dimensional Parameter Values for Fig. 3

Physical parameter	Value
E_u	30,000 MPa
E_l	20,000 MPa
G_a	400 MPa
h_u	6 mm
h_l	6 mm
h_a	0.1 mm
L_u	100 mm
L_l	100 mm
c	95 mm
P	1,000 N/mm
Computed parameter	**Value**
α_1	$1.04 \cdot 10^{-1}$ 1/mm^2
α_2	$1.89 \cdot 10^{-2}$ 1/mm^3
η_1	$2.13 \cdot 10^{-2}$ 1/mm^4
η_2	$4.80 \cdot 10^{-2}$ 1/mm^3
A_1	$8.61 \cdot 10^{-1}$ N/mm^3
A_2	$7.10 \cdot 10^{-1}$ N/mm^3
B_1	$3.63 \cdot 10^{-1}$ N/mm^7
B_2	$4.13 \cdot 10^{-2}$ N/mm^7
B_3	$1.56 \cdot 10^{-2}$ N/mm^8
B_4	$6.88 \cdot 10^{-4}$ N/mm^8

Note: Details are given in the note for Table 1. The computed parameters are not referenced within the text.

problems such as the model in Yuceoglu and Updike (1980), which includes the effects of shear deformations but was limited to a numerical study because of its complexity. Application of the method presented could be used to directly examine how shear deformations contribute to the boundary layer zone features.

References

Banks-Sills, L., and Salganik, R. (1994). “An asymptotic approach applied to a longitudinal crack in an adhesive layer.” *Int. J. Fract.*, 68(1), 55–73.

Barenblatt, G. I. (1996). *Scaling, self-similarity, and intermediate asymptotics*, Cambridge University Press, New York.

Bender, C. M., and Orzsag, S. A. (1978). *Advanced mathematical methods for scientists and engineers*, McGraw Hill, New York.

Gilibert, Y., and Rigolot, A. (1988). “Determination of stress distribution in double lap joints, matched asymptotic expansions and conformal mapping.” *Adhesively Bonded Joints: Testing, Analysis, and Design, ASTM STP 981*, ASTM, West Conshohoken, PA, 145–159.

Gustafson, P. A., Bizard, A., and Waas, A. M. (2007). “Dimensionless parameters in symmetric double lap joints: An orthotropic solution for thermomechanical loading.” *Int. J. Solids and Structures*, 44(17), 5774–5795.

Hassan, E., Kalamkarov, A. L., and Georgiades, A. (2009). “An asymptotic homogenization model for smart 3D grid-reinforced composite structures with generally orthotropic constituents.” *Smart Mater. Struct.*, 18(7).

J. Eng. Mech., 2013, 139(10): 1387-1394

Kevorkian, J., and Cole, J. D. (1975). *Perturbation methods in applied mathematics*, Springer, New York.

Klarbring, A., and Movchan, A. (1998). "Asymptotic modelling of adhesive joints." *Mech. Mater.*, 28(1–4), 137–145.

Li, G. (2000). "Deformations of balanced and unbalanced adhesively bonded single-lap joints." Ph.D. thesis, Univ. of New Brunswick, Fredericton, NB, Canada.

Shahin, K., Kember, G., and Taheri, F. (2008). "An asymptotic solution for evaluation of stresses in balanced and unbalanced adhesively bonded joints." *Mech. Adv. Mater. Struct.*, 15(2), 88–103.

Van Dyke, M. (1975). *Perturbation methods in fluid mechanics*, Parabolic Press, Stanford, CA.

Yuceoglu, U., and Updike, D. P. (1980). "Stress analysis of bonded plates and joints." *J. Engrg. Mech. Div.*, 106(1), 37–56.

J. Eng. Mech., 2013, 139(10): 1387-1394